### Title
Noninvasive Imaging Techniques for Monitoring Cellular Response to Treatment in Stable Vitiligo




### Journal
Journal of Investigative Dermatology, 144(4)

### ISSN
0022-202X



### Authors
Shiu, Jessica
Lentsch, Griffin
Polleys, Christopher M
et al.



### Publication Date
2024-04-01

### DOI
10.1016/j.jid.2023.10.006

# Noninvasive Imaging Techniques for Monitoring Cellular Response to Treatment in Stable Vitiligo

JID Open

*Journal of Investigative Dermatology* (2023) ■, ■–■; doi:10.1016/j.jid.2023.10.006

## TO THE EDITOR

Vitiligo, an immune-mediated melanocyte destruction disorder (Harris, 2018), is often treated with immunomodulators and phototherapy (Bae et al, 2017). Surgical interventions can achieve 45%–47% success with >90% repigmentation (Ju et al, 2021) in stable vitiligo, but responses are unpredictable (Rajaram et al, 2017). Quantifying vitiligo treatment response to grafting is challenging because of the limited sensitivity of the Vitiligo Area Scoring Index (Gan et al, 2017; Komen et al, 2015), which can only capture macroscopic changes after 6–12 months (Gao et al, 2022). Reflectance confocal microscopy (RCM) and multiphoton microscopy (MPM) are noninvasive techniques for cellular-level skin imaging without labeling (Lentsch et al, 2022; Tkaczyk, 2017). RCM has been used to measure vitiligo treatment responses (Ardigo et al, 2007). MPM, which detects cellular metabolic changes via two-photon excitation fluorescence from reduced NADH (Pouli et al, 2016), has identified keratinocyte metabolic changes associated with vitiligo disease persistence (Shiu et al, 2022). Although MPM can visualize NADH contrast, existing clinical devices have a submillimeter scale field of view. Combining MPM with RCM can overcome this limitation (Lentsch et al, 2022). This approach has not been applied to vitiligo, in which this combination approach may be particularly useful for measuring keratinocyte metabolism changes and melanocyte migration simultaneously.

We evaluated vitiligo punch grafting effectiveness using MPM and RCM imaging on 12 stable vitiligo lesions in 11 patients (Supplementary Materials and Methods) over 5 visits (baseline, 1, 3, 6, and 10 weeks after treatment). Patients who received treatment had stable lesions for over a year, were unresponsive to prior treatments, and had a 3-month treatment washout. Patients provided written informed consent to participate in the study, which was approved by the University of California, Irvine Institutional Review Board. Vivascope1500 (CaliberID) and MPTflex (JenLab GmbH) were used for in vivo RCM and MPM imaging, respectively. We acquired images as described previously (Lentsch et al, 2022; Shiu et al, 2022) (see Supplementary Materials and Methods for details). RCM was performed at weeks 3 and 6 for 8 of the 12 lesions and at week 10 for 11 of the 12 lesions owing to device availability and participant dropout. Consistency was maintained by imaging the same graft at each visit to correlate optical biomarkers of melanocyte migration and keratinocyte metabolic changes with treatment responses.

RCM measured melanocyte density (number of melanocytes per unit area) and distance from the graft site. Five of the 12 lesions showed clinical repigmentation by week 10. Activated melanocytes with bipolar and/or stellate dendrites in patients showing clinical repigmentation were seen as early as 3 weeks in 2 patients and 6 weeks in most patients (Figure 1a and c), their appearance preceded clinical evidence of repigmentation, and their density increased over time (statistical significance was not determined secondary to the sample size). Nonresponders lacked activated melanocytes, consistent with prior findings identifying melanocyte activation's repigmentation role (Abdallah et al, 2003), and visualized melanocyte count was significantly higher in responders (mean = 4.8, SD = 2.6) versus in nonresponders (mean = 0, SD = 0). Melanocyte distance from the graft increased in most responsive patients (Figure 1b), suggesting melanocyte migration. Patients in whom melanocytes were imaged did not exhibit later disappearance of melanocytes, suggesting that the lack of response was not due to melanocyte destruction.

MPM can capture keratinocyte pigmentation and melanocyte migration changes after punch grafting in vitiligo (Figure 2a–e), but the limited field of view precludes accurate measurement of melanocyte density or migration. MPM images obtained from different epidermal depths within the same graft throughout the treatment were used to quantitatively assess metabolic changes using mitochondrial clustering analysis (Pouli et al, 2016) (Supplementary Materials and Methods). Baseline imaging of the normal skin before treatment exhibits depth-dependent changes in mitochondrial clustering (β), reflecting differences in metabolism. Basal and parabasal keratinocytes have higher β values compared with keratinocytes in higher epidermal layers as keratinocytes transition from glycolysis to oxidative phosphorylation during cell differentiation, progressing from a more fragmented mitochondria phenotype in the basal layer to a more fused phenotype in higher epidermal layers (Supplementary Figure S1) (Pouli et al, 2016). β values indicated altered keratinocyte metabolism in vitiligo lesions compared with the perilesional skin for all patients at baseline. Comparing the same metric at different treatment visits, basal keratinocytes in responsive vitiligo skin reverted to a more glycolytic profile within 6 weeks. In contrast, basal keratinocytes in nonresponsive lesions remained metabolically distinct from the adjacent normal skin (Figure 2f). β variability across the responsive

*Abbreviations: MPM, multiphoton microscopy; RCM, reflectance confocal microscopy*

*Accepted manuscript published online XXX; corrected proof published online XXX*

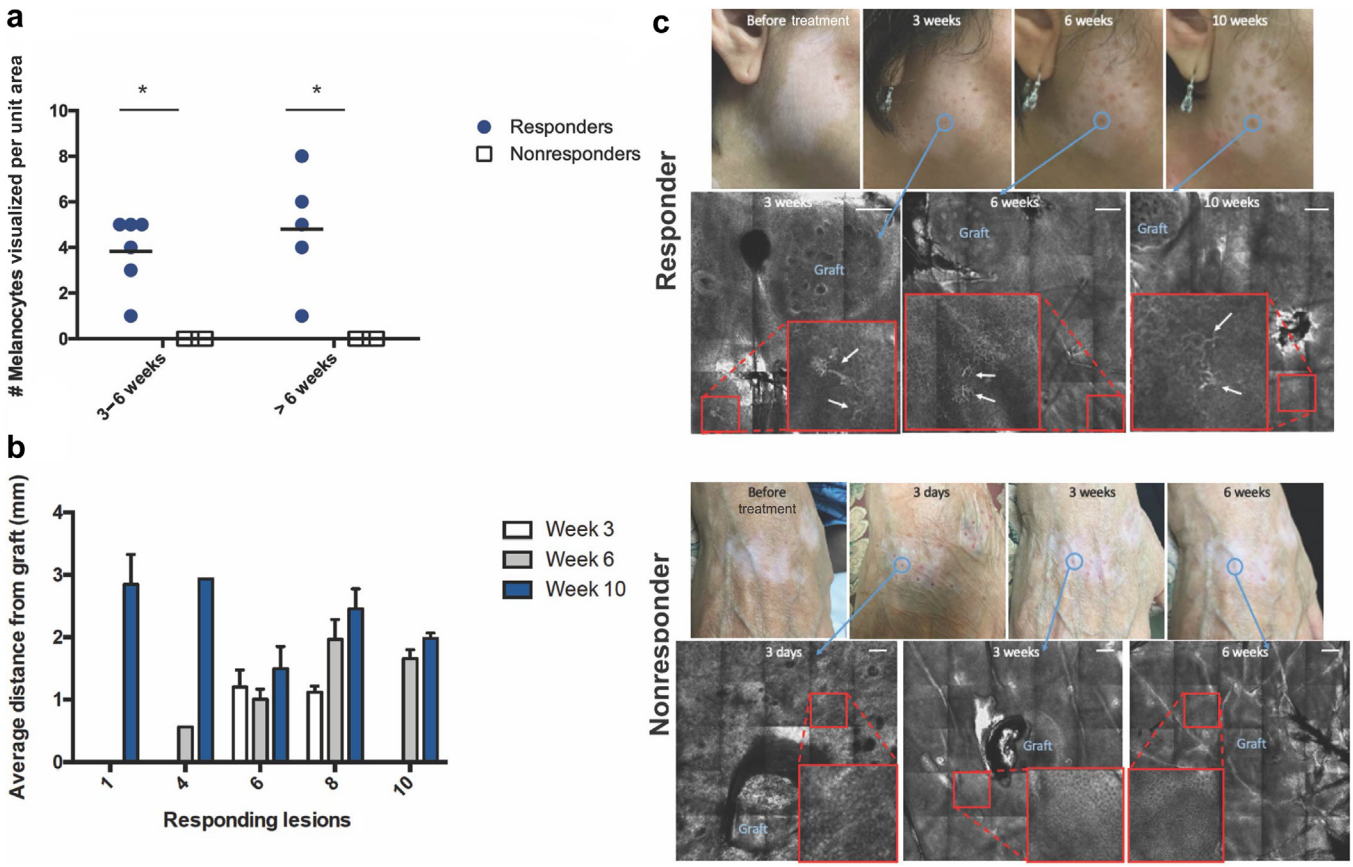


**Figure 1. In vivo RCM imaging following vitiligo treatment enables melanocyte quantification.** (**a**) Melanocyte density in responders and nonresponders at different visits. Each data point represents number of activated melanocytes visualized in a lesion per unit area per visit. **P*-value < .05. (**b**) Average distance per melanocyte from punch graft in treatment responders. (**c**) Blue circle depicts clinical area that was imaged over time and the corresponding RCM image. Enlarged views of the area of interest are depicted in large red squares. Activated melanocytes are indicated by white arrows. Scale bars = 200 μm.

vitiligo epidermis aligned with the nonlesional skin by 6 weeks, remaining consistent after 10 weeks (Figure 2g). Metabolic profile differences between keratinocytes in the lesional and nonlesional skin were insignificant in responders at 6 weeks but persisted in nonresponders beyond 10 weeks after the treatment. These findings suggest that keratinocyte metabolism shifts may serve as a potential indicator of treatment response failure. β variability values were compared using a linear mixed-effects model generated in SAS JMP Pro 14 (Supplementary Materials and Methods).

In this study, we used RCM and MPM to monitor vitiligo treatment response at a cellular level, identifying changes in melanocyte morphology and keratinocyte metabolism that correlate with an early response. Melanocyte activation emerges as an early treatment response indicator, observed as early as 3 weeks after treatment initiation, preceding clinical repigmentation. Absence of melanocyte activation in nonresponders suggests that treatment failure is a consequence of lack of melanocyte activation rather than immune-mediated melanocyte destruction. However, it is possible that a small immune infiltrate went unnoticed, either because of limitations in detecting low-level T-cell responses or the study's small sample size.

Although these results highlight the potential of noninvasive optical microscopy in predicting tissue-level responses that align with therapeutic outcomes, we acknowledge that the combination of MPM and RCM is time-consuming, which may limit its clinical applicability. Promising advances such as the fast, large area multiphoton exoscope (Fast et al, 2020), which can simultaneously gauge local tissue metabolic changes and melanocyte activation, holds potential for capturing and understanding early cytologic treatment responses in vitiligo, a crucial aspect in determining why some lesions respond to treatment while others do not. Future studies using fast, large area multiphoton exoscope on a larger group of patients with vitiligo will help validate our current findings and further establish the utility of in vivo nonlinear optical microscopy for monitoring local cytological responses to therapy.

## Data availability statement

No large datasets were generated from these data. The data that support the findings of this study are available from the corresponding author (JS) upon reasonable request.

**KEYWORDS**
Keratinocyte; Melanocyte; Multiphoton microscopy; Reflectance confocal microscopy; Vitiligo

**ORCIDs**
Jessica Shiu: https://orcid.org/0000-0002-2264-8372
Griffin Lentsch: https://orcid.org/0000-0003-2465-9937
Christopher M. Polleys: https://orcid.org/0009-0006-0263-9395
Pezhman Mobasher: https://orcid.org/0000-0002-8737-3373

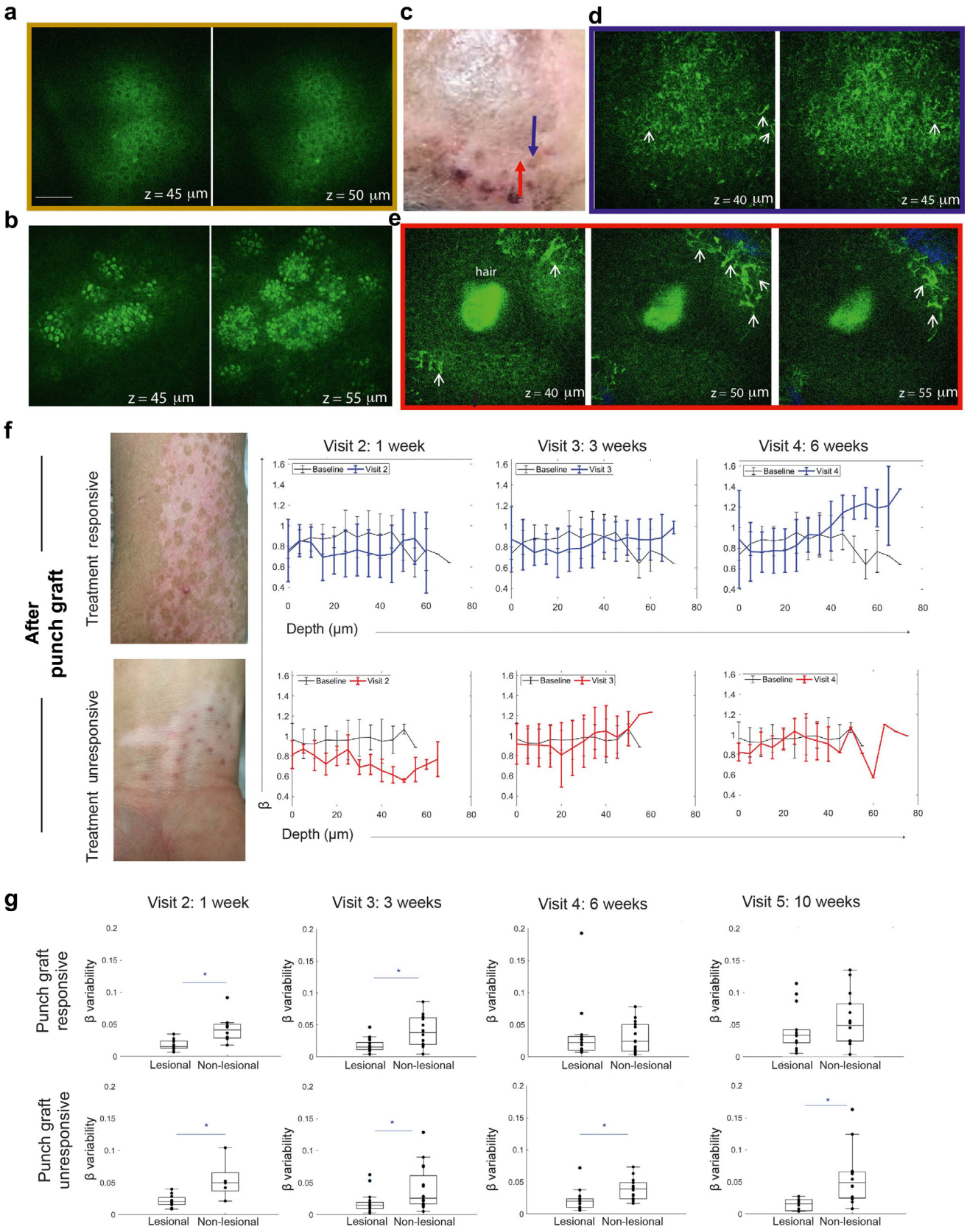


**Figure 2. In vivo MPM imaging after vitiligo treatment captures repigmentation and metabolic changes.** MPM images showing nonpigmented keratinocytes in lesional acceptor (**a**) and melanin caps in nonlesional donor skin (**b**); (**c**) Clinical image of the imaged graft (blue arrow) and adjacent imaged location (red arrows). (**d, e**) MPM images showing activated melanocytes (arrows) in graft (**c**) and migrating melanocytes in a hair follicle in adjacent location. (**f**) Clinical images of treated areas and spline fits of β values showing basal keratinocytes reverting to a more glycolytic profile within 6 weeks in responders, while maintaining a distinct profile from normal skin in nonresponders. (**g**) β variability values of keratinocytes in treated vitiligo aligning with nonlesional skin for responders by 6 weeks. *$P$-value $< .05$.

Marissa Ericson: https://orcid.org/0000-0003-0385-2797
Irene Georgakoudi: https://orcid.org/0000-0002-0049-6697
Anand K. Ganesan: https://orcid.org/0000-0003-4944-9274
Mihaela Balu: https://orcid.org/0000-0002-8018-5134

## CONFLICT OF INTEREST

MB is coauthor of a patent owned by the University of California, Irvine (UCI), which is related to multiphoton microscopy (MPM) imaging technology. MB is cofounder of Infraderm, LLC, a startup spin-off from the UCI, which develops MPM-based clinical imaging platforms for commercialization purposes. The Institutional Review Board and Conflict of Interest Office of the UCI have reviewed patent disclosures and did not find any concerns. The rest of the authors state no conflict of interest.

## ACKNOWLEDGMENTS

JS acknowledges the grant support from the NIH (5KL2TR1416-6), NIAMS (K08AR081406), and seed grant support from the Skin Biology Resource-Based Center, University of California, Irvine (P3011935106). MB, AKG, and IG acknowledge the grant support from NIBIB (R01EB026705). MB and AKG also acknowledge the grant support from NIAMS (R21AR073408) and from the Skin Biology Resource-Based Center, University of California, Irvine (P3011935106).

## AUTHOR CONTRIBUTIONS

Conceptualization: MB, AKG, IG; Data Curation: JS, GL, CMP, PM; Formal Analysis: JS, GL, CMP, PM, ME; Funding Acquisition: JS, MB, IG, AKG; Investigation: GL, CMP; Methodology: MB, IG, AKG; Project Administration: JS, GL, PM, AKG, IG, MB; Resources: JS, MB, AKG; Software: GL, CMP; Supervision: IG, MB, AKG; Validation: JS, GL, CMP, IG, AKG, MB; Visualization: JS, GL, CMP; Writing - Original Draft Preparation: JS, GL, MB; Writing - Review and Editing: JS, GL, CMP, IG, MB, AKG

***Jessica Shiu*[1,*,7], *Griffin Lentsch*[2,7], *Christopher M. Polleys*[3,7], *Pezhman Mobasher*[1], *Marissa Ericson*[4], *Irene Georgakoudi*[3,8], *Anand K. Ganesan*[1,5,6,8] and *Mihaela Balu*[2,6,8]**

[1]*Department of Dermatology, University of California, Irvine, Irvine, California, USA;* [2]*Beckman Laser Institute and Medical Clinic, University of California, Irvine, Irvine, California, USA;* [3]*Department of Biomedical Engineering, Tufts University, Medford, Massachusetts, USA;* [4]*Biostatistics, Epidemiology and Research Design, University of California, Irvine, Irvine, California, USA;* [5]*Department of Biological Chemistry, University of California, Irvine, Irvine, California, USA; and* [6]*Skin Biology Resource Center, University of California, Irvine, Irvine, California, USA*

[7]*These authors contributed equally to this work.*
[8]*These authors share senior authorship.*

[*]*Corresponding author e-mail: jshiu1@uci.edu*

## SUPPLEMENTARY MATERIAL

Supplementary material is linked to the online version of the paper at www.jidonline.org, and at https://doi.org/10.1016/j.jid.2023.10.006.

## REFERENCES

Abdallah M, Abdel-Naser MB, Moussa MH, Assaf C, Orfanos CE. Sequential immunohistochemical study of depigmenting and repigmenting minigrafts in vitiligo. Eur J Dermatol 2003;13:548–52.

Ardigo M, Malizewsky I, Dell'anna ML, Berardesca E, Picardo M. Preliminary evaluation of vitiligo using in vivo reflectance confocal microscopy. J Eur Acad Dermatol Venereol 2007;21:1344–50.

Bae JM, Jung HM, Hong BY, Lee JH, Choi WJ, Lee JH, et al. Phototherapy for vitiligo: a systematic review and meta-analysis. JAMA Dermatol 2017;153:666–74.

Fast A, Lal A, Durkin AF, Lentsch G, Harris RM, Zachary CB, et al. Fast, large area multiphoton exoscope (FLAME) for macroscopic imaging with microscopic resolution of human skin. Sci Rep 2020;10:18093.

Gan EY, Eleftheriadou V, Esmat S, Hamzavi I, Passeron T, Böhm M, et al. Repigmentation in vitiligo: position paper of the Vitiligo Global Issues Consensus Conference. Pigment Cell Melanoma Res 2017;30:28–40.

Gao PR, Wang CH, Lin YJ, Huang YH, Chang YC, Chung WH, et al. A comparative study of suction blister epidermal grafting and automated blister epidermal micrograft in stable vitiligo. Sci Rep 2022;12:393.

Harris J. Vitiligo's impact is in the eye of the beholder. Nature 2018;563:S99.

Ju HJ, Bae JM, Lee RW, Kim SH, Parsad D, Pourang A, et al. Surgical interventions for patients with vitiligo: a systematic review and meta-analysis. JAMA Dermatol 2021;157:307–16.

Komen L, da Graça V, Wolkerstorfer A, de Rie MA, Terwee CB, van der Veen JP. Vitiligo Area Scoring Index and Vitiligo European Task Force assessment: reliable and responsive instruments to measure the degree of depigmentation in vitiligo. Br J Dermatol 2015;172:437–43.

Lentsch G, Baugh EG, Lee B, Aszterbaum M, Zachary CB, Kelly KM, et al. Research Techniques Made Simple: emerging imaging technologies for noninvasive optical biopsy of human skin. J Invest Dermatol 2022;142:1243–1252.e1.

Pouli D, Balu M, Alonzo CA, Liu Z, Quinn KP, Rius-Diaz F, et al. Imaging mitochondrial dynamics in human skin reveals depth-dependent hypoxia and malignant potential for diagnosis. Sci Transl Med 2016;8:367ra169.

Rajaram M, Alagarsamy S, Sundarapandiyan S. Post punch graft appearance of repigmentation time in stable vitiligo: a retrospective study. Int J Sci Study 2017;5:4.

Shiu J, Zhang L, Lentsch G, Flesher JL, Jin S, Polleys C, et al. Multimodal analyses of vitiligo skin identify tissue characteristics of stable disease. JCI Insight 2022;7:e154585.

Tkaczyk E. Innovations and developments in dermatologic non-invasive optical imaging and potential clinical applications. Acta Derm Venereol 2017;Suppl 218:5–13.

## SUPPLEMENTARY MATERIALS AND METHODS

### Patient characteristics

A total of 11 patients, aged 20 to 74 years, with stable vitiligo were enrolled in this study with 12 lesions imaged (Institutional Review Board #2018-4362). The vitiligo lesions were distributed across various locations, including wrist (2), hand (2), leg (5), arm (1), back (1), and face (1). Imaging sessions took place at baseline (before treatment initiation) and at 3, 6, and 10 weeks after the punch grafting and narrow-band UVB treatment.

### Reflectance confocal microscopy image acquisition

The reflectance confocal microscopy images were acquired as z-stacks of en-face images, spanning from the stratum corneum to the superficial dermis with a 5-μm step size. The tile mosaics of en-face images were acquired, encompassing up to 6 × 6 $mm^2$ areas, with each individual en-face image having a field of view of 500 × 500 $\mu m^2$.

### Multiphoton microscopy image acquisition

Multiphoton microscopy data were acquired as z-stacks of en-face images spanning from the stratum corneum to the superficial dermis with a 5-μm step. Each optical section had a field of view of 100 × 100 $\mu m^2$.

### Mitochondrial clustering analysis

Mitochondrial clustering was quantified using a previously described Fourier-based approach in which the intensity variations of a two-photon excitation fluorescence image are attributed to variations in mitochondrial NADH binding. Mitochondrial clustering, or β, was extracted from each image by analyzing the intensity variations isolated from the cellular cytoplasm. In brief, autofluorescence contributions from keratin, melanin, nuclei, interstitial space, and dermis (as identified via a collagen second-harmonic generation signal) were masked. Contrast-limited adaptive histogram equalization was applied to the two-photon excitation fluorescence and second-harmonic generation images, and features were subsequently segmented using Otsu's global thresholding. The mask was finalized by applying a median filter to remove noise and taking the complement of the image to mask features corresponding to the segmented signal. This approach was validated by demonstrating that dynamic changes in mitochondrial clustering of human skin epithelia confined to the basal layer in response to hypoxia were consistent with an expected enhancement in the relative levels of glycolysis (Pouli et al, 2016). β variability values were compared using a linear mixed-effects model generated in SAS JMP Pro 14. Fixed effects included treatment responsiveness, imaging location, and visit number, whereas random effects encompassed patient number and z-stack number. Pairwise comparisons using a post hoc Tukey honest significant difference test found significance at a level of $\alpha = 0.05$.

## SUPPLEMENTARY REFERENCE

Pouli D, Balu M, Alonzo CA, Liu Z, Quinn KP, Rius-Diaz F, et al. Imaging mitochondrial dynamics in human skin reveals depth-dependent hypoxia and malignant potential for diagnosis. Sci Transl Med 2016;8:367ra169.

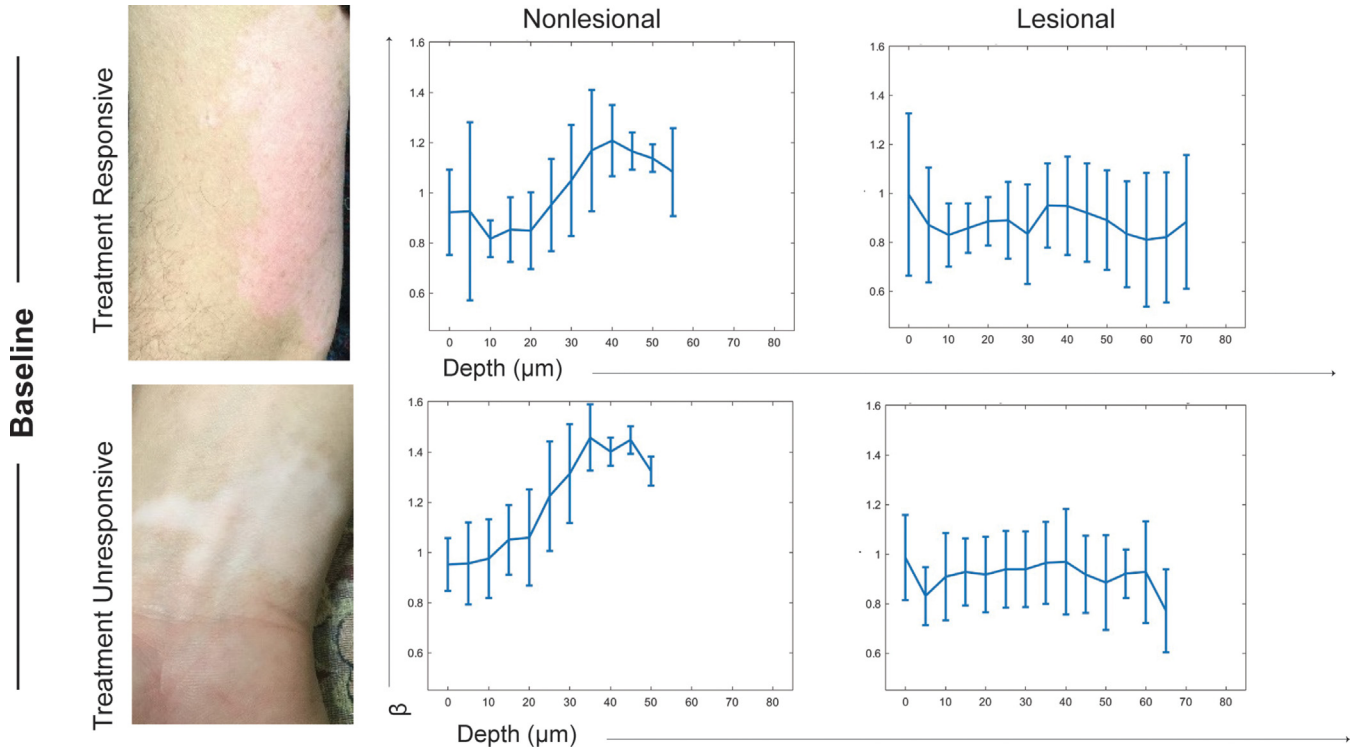


**Supplementary Figure S1. In vivo MPM baseline imaging of the vitiligo skin before punch grafting treatment.** Representative baseline clinical images from patients with vitiligo undergoing punch grafting in treatment responders and nonresponders. Average mitochondrial clustering (β) values based on z-stacks from 12 vitiligo lesions as a function of depth at baseline are shown as spline fits. MPM, multiphoton microscopy.